diversity

MDPI

Article

Genome-Wide Analysis of SPL Gene Families Illuminate the Evolution Patterns in Three Rubber-Producing Plants

Renping Su [1], Boxuan Yuan [1], Yang Yang [2], Guoen Ao [1] and Juanying Wang [1,*]

[1] The Key Laboratory of Plant Resource Conservation and Germplasm Innovation in Mountainous Region (Ministry of Education), Institute of Agro-Bioengineering, College of Life Sciences, Guizhou University, Guiyang 550025, China; ls.rpsu20@gzu.edu.cn (R.S.); yuanboxuan111@163.com (B.Y.); aoguoen@163.com (G.A.)

[2] College of Life Sciences, Hainan Normal University, Haikou 571158, China; 15776580499@163.com

* Correspondence: juanying020@163.com; Tel.: +86-133-3842-2948

Abstract: Transcription factors SQUAMOSA Promoter-binding Protein-like (SPL) play a crucial role in regulating plant response to stress, root development, and flower production. However, analysis of SPL gene families in the three rubber-producing plants *Taraxacum kok-saghyz*, *Hevea brasiliensis*, and *Eucommia ulmoides*, renowned for their natural rubber production, has not yet been conducted. In this study, we utilized reference genomes to perform genome-wide analysis, and obtained new insights on the evolution of SPL gene families in these three rubber-producing plants. Our results revealed the following: (1) *T. kok-saghyz*, *H. brasiliensis*, and *E. ulmoides* harbored 25, 16, and 13 SPL genes, respectively, containing conserved structural domains of SBP. (2) A phylogenetic analysis categorized 90 SPL proteins from 25 TkSPLs, 16 HbSPLs, 13 EuSPLs, 17 AtSPLs, and 19 OsSPLs into eight groups. (3) Analysis of cis-acting elements demonstrated that the promoters of EuSPLs contained a significant number of light response elements, hormone regulatory elements, and stress response elements. (4) Transcriptome data analysis revealed that the EuSPL8 gene had strong expression in bark, as well as TkSPL4 and TkSPL8 exhibit high expression levels specifically in roots and latex. This study provides valuable insights into the biological functions of the SPL gene family in the three rubber plants and might serve as a reference for identifying efficient genes.

Keywords: *Taraxacum kok-saghyz*; *Hevea brasiliensis*; *Eucommia ulmoides*; genome-wide; SPLs; expression pattern

Citation: Su, R.; Yuan, B.; Yang, Y.; Ao, G.; Wang, J. Genome-Wide Analysis of SPL Gene Families Illuminate the Evolution Patterns in Three Rubber-Producing Plants. *Diversity* **2023**, *15*, 983. https://doi.org/10.3390/d15090983

Academic Editors: Hong-Hu Meng and Yi-Gang Song

Received: 13 July 2023
Revised: 22 August 2023
Accepted: 23 August 2023
Published: 31 August 2023

1. Introduction

Transcription factors (TFs), a crucial subclass of regulatory proteins that control gene expression, are vital for plant growth and development because they bind to cis-acting areas to either activate or inhibit the production of downstream genes. SQUAMOSA Promoter-binding Protein-like (SPL) proteins are a family of plant-specific TFs with a highly conserved DNA-binding SBP domain made up of two distinct zinc finger architectures, Zn-1 (Cys3Hes or Cys4) and Zn-2 (Cys2HisCys) [1] Since the SBP genes AmSBP1 and AmSBP2 were discovered for the first time in *Antirrhinum majus* [2], the genome-wide analysis of the SPL gene family has now been performed for numerous species, including 12 SPLs in sweet cherry (*Prunus avium* L.) [3], 23 SPLs in quinoa (*Chenopodium quinoa* Willd.) [4], and 18 SPLs in foxtail millet (*Setaria italica*) [5]. As more plant genomic resources become available, more SPL genes will probably be found.

SPL transcription factors are crucial regulators of plant growth, development, and stress response. The microRNA-targeted transcription factor SPL3, which initiates and subsequently activates the transcription factors LEAFY, FRUITFULL, and APETALA1, controls the time of flower development in *Arabidopsis* [6]. Early blooming in *Arabidopsis* was reportedly stopped by AtSPL3 [7]. AtSPL8 appears to be implicated in gibberellin signaling, according to an overexpression study [8]. SPL genes control the homeostasis of copper (Cu)

and the response to Cu deficiency [9,10], and cadmium (Cd) tolerance [11,12]; they take part in hormone signaling as well as reactions to a variety of biotic and abiotic stimuli, including as heat, cold, salt, thirst, and injury [13–16]. AtSPL9 and AtSPL15 play complementary roles in controlling plastochron length and shoot maturation [17,18], and AtSPL9-controlled cell elongation and the transition from the vegetative phase through the BR (brassinosteroid) signaling pathway [19]. SPL genes are essential for phase transitions in addition to the roles they perform in the aforementioned processes [20,21], latitudinal root growth [22], trichome development [23–25], embryogenesis [26], and seedling growth [27]. SPL genes control rice grain shape, size, quality, and yield in addition to plant architecture [28–31].

Natural rubber, with distinct physical characteristics [32,33], is a valuable industrial raw material used extensively in the transportation, medicinal, and defense sectors. Currently, the prevalent plants that produce rubber are *Hevea brasiliensis*, *Taraxacum kok-saghyz*, and *Eucommia ulmoides* [33,34]. Several TFs participate in the control of the expression of the genes involved in rubber biosynthesis in *H. brasiliensis*. As an example, the expression of HbSRPP was decreased by the three genes HbWRKY14, HbWRKY1, and HbMADS4 [35,36]. HbFPS1 expression was increased by HblMYB19, HblMYB44, and HbWRKY27 [37,38]. HbRZFP1 decreased the expression of HRT2 [39]. HbMYC2b controls the expression of HbSRPP [40]. While TkWRKY21 was up-regulated under heat stress, TkWRKY18, TkWRKY23, and TkWRKY38 were all considerably up-regulated during cold stress [41]. The majority of CBF genes in TKS seedlings that had undergone cold acclimation took longer to react to the cold signal than those that had not [42]. Most of the EuWRKYs genes were highly expressed in leaf buds and involved in leaf development [43]. The genes EuMADS39 and EuMADS65 were highly expressed in male individuals, whether in flower or leaf tissues [44]. These findings demonstrated that TFs are essential for rubber biosynthesis.

However, the precise role of SPL genes in rubber biosynthesis remains incompletely understood in these three rubber-producing plants. Despite that, it is believed that they may regulate the expression of genes involved in either the mevalonate (MVA) pathway or the methylerythritol phosphate (MEP) pathway, both of which contribute to the synthesis of the isoprenoid precursor for rubber molecules. Therefore, we selected three significant natural rubber producers, *H. brasiliensis*, *T. kok-saghyz*, and *E. ulmoides*. In this study, a thorough analysis of the gene structure, conserved domain, chromosome location, cis-acting element, and expression pattern of the SPL genes in three rubber-producing plants was conducted in this study. Through analyzing the SPL gene family in these plants, our objective was to gain potential insights into the involvement of SPL genes in the biosynthesis of natural rubber.

2. Materials and Methods

2.1. SPL Identification across the Genome and Phylogenetic Analysis

The genomic sequences of *T. kok-saghyz*, *H. brasiliensis*, and *E. ulmoides* were retrieved from the NCBI and Genomic Warehouse databases (https://ngdc.cncb.ac.cn, accessed on 23 April 2023). This study used the Phytozome (https://phytozome-next.jgi.doe.gov, accessed on 23 April 2023) database to download the AtSPLs and OsSPLs protein sequences that are used to retrieve the protein sequences of *T. kok-saghyz*, *H. brasiliensis*, and *E. ulmoides*. The SBP domain sequences (ID: PF03110) from the Pfam database were used to scan the three genome sequences of rubber-producing plants for putative SPL genes using HMMER (http://hmmer.org, accessed on 23 April 2023). The local BLAST and hidden Markov models were utilized for comparison in order to locate the SPL family members in all three species, and the findings were combined. Delete domain-less or domain-incomplete sequences manually to guarantee the accuracy of the results. The first transcript is chosen as the typical sequence in situations when there are numerous transcripts of the same gene. The protein domain was analyzed by NCBI Batch CD-search and plotted by Chiplot's website (https://www.ncbi.nlm.nih.gov/Structure/bwrpsb/bwrpsb.cgi and https://www.chiplot.online/, accessed on 23 April 2023). Gene mapping was performed using TBtools software (https://github.com/CJ-Chen/TBtools/releases, accessed on 23 April 2023).

The amino acid sequences of *T. kok-saghyz*, *H. brasiliensis*, *E. ulmoides*, *Oryza sativa* and *Arabidopsis thaliana* SPLs were compared in multiple sequences using ClustalW 2.0 software, while the phylogenetic tree was built using the neighbor-joining method with MEGA 11.0 software, with the number of replications set at 1000 and all parameters left at their default settings, and figures with confidence levels below 60 were selected to be hidden in Figure 1 and, finally, touched up in the iTQL website (https://itol.embl.de, accessed on 23 April 2023).

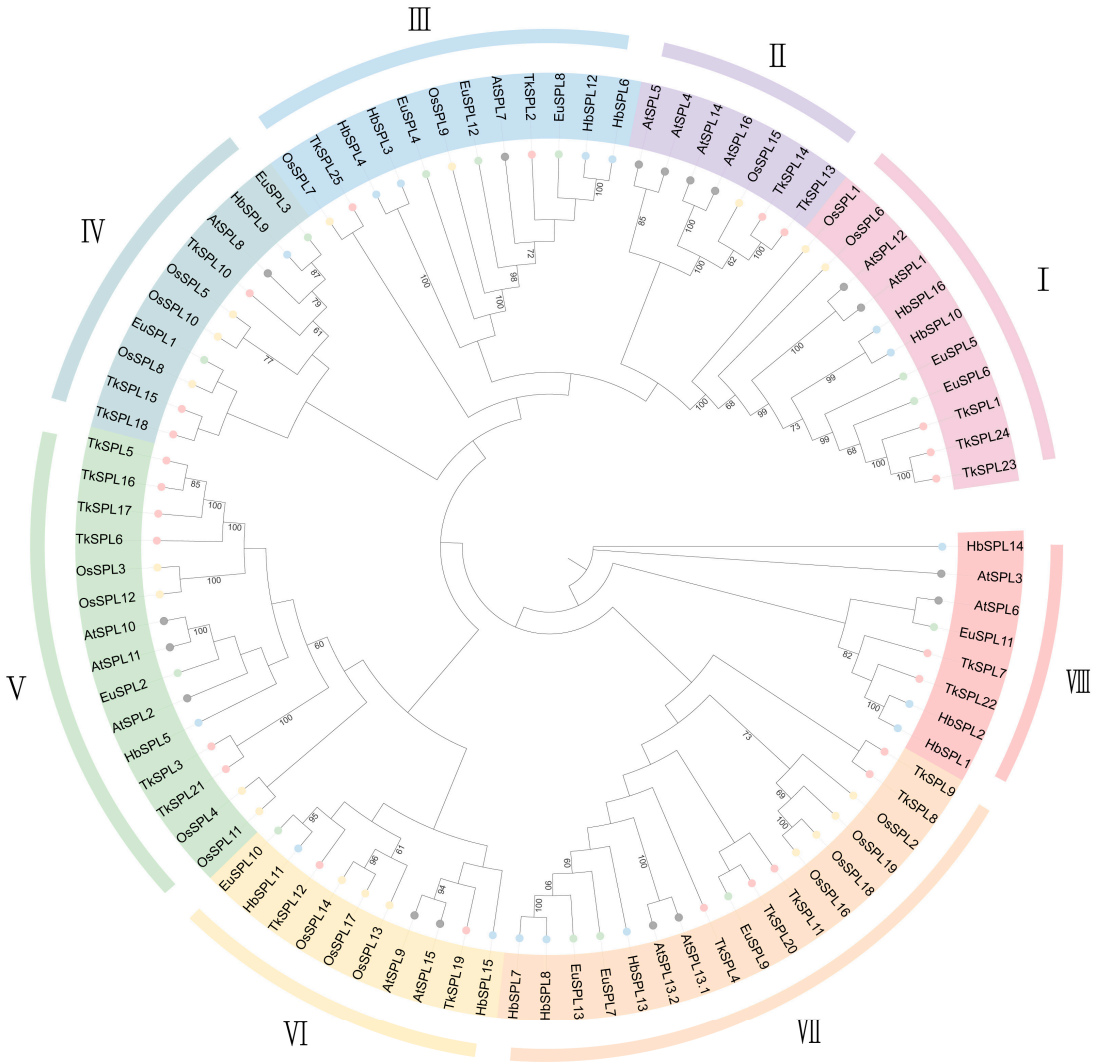

Figure 1. Phylogenetic tree includes 90 SPLs from 5 different plants. Using MEGA 11.0 and the neighbor-joining (NJ) method, a phylogenetic tree based on the SBP domain was created. The bootstrap value is represented by the number of branches.

2.2. Physicochemical Characterization and Structural Analysis of the Protein

The amino acid count, relative molecular weight, theoretical isoelectric point, and instability index of TkSPLs, HbSPLs, and EuSPLs were examined using the ExPASy Prot Param program (https://web.expasy.org/protparam/, accessed on 23 April 2023). By comparing SPL gene sequences to the matching genomic DNA sequences, the exons, introns, CDS, and UTRs of the genes were identified. WoLF PSORT (https://wolfpsort.hgc.jp, accessed on 23 April 2023) is used to predict protein subcellular localization. Expasy and TMHMM-2.0 were used to assess the hydrophobicity and transmembrane characteristics of proteins (https://web.expasy.org/protscale/ and https://ser-vices.healthtech.dtu.dk/Services/TMHMM-2.0/, accessed on 23 April 2023). The secondary and tertiary structures of proteins can be predicted using the SOPMA and Phyre2 programs (https://npsa-prabi.

ibcp.fr/cgi-bin/npsa_automat.pl?page=npsa_sopma.html and http://www.sbg.bio.ic.ac.uk/phyre2/html/page.cgi?id=index, accessed on 23 April 2023).

2.3. Analysis of Protein Domains and Conserved Motifs

Using ClustalW 2.0, the protein sequences of AtSPL, OsSPL, and the 54 SPL sequences discovered in this investigation were aligned to identify the SBP domain [45]. TBtools was used to examine the exon–intron structure [46], using the genome and cDNA sequences of the SPL gene retrieved from the genomes of four rubber-producing plants. Three rubber-producing plant gene family members were subjected to protein motif analysis using the web program MEME (https://meme-suite.org/meme/tools/meme, accessed on 25 April 2023) [47]. This analysis used up to 10 motlets and other default parameters. Using GFF files of three rubber-producing plants and two model plants, as well as the files of the previous construction of the evolutionary tree, the gene structure and motif combination map were drawn on the TBtools software. The PlantCare website (http://bioinformatics.psb.ugent.be/webtools/plantcare/html/, accessed on 25 April 2023) was used to predict the cis-acting elements in the promoter region of the three rubber-producing plant SPLs using the 2000 bp sequence upstream of the translation start codon (ATG), and the TBtools software was then used for visual analysis.

2.4. Collinearity Analysis

The genome sequences of Oryza sativa and *Arabidopsis* thaliana were downloaded from Phytozome (https://phytozome-next.jgi.doe.gov, accessed on 23 April 2023) to create a chromosome location and collinearity plot in order to analyze the replication patterns and evolutionary mechanisms of SPL genes.

2.5. Analysis of Expression Patterns across Several Developmental Stages and Tissue Types

The NCBI database was used to download the transcriptome information for various tissues and time periods in *E. ulmoides*, the relative expression abundance of SPLs of the three rubber-producing plants was expressed by FPKM value, the logarithm of the value was statistically analyzed, and the TBtools software generated a heat map of gene expression, where the highest expression was denoted by a red box and the lowest expression by a blue box.

3. Results

3.1. SPL Identification across the Genome and Phylogenetic Analysis

Local BLAST and the hidden Markov model were utilized for screening purposes, resulting in the identification of 25 TkSPLs, 16 HbSPLs, and 13 EuSPLs (Table 1). The Supplementary Materials provide information on the SBP domain and gene localization of these three species following the identification and screening process (Figures S1 and S2).

To enhance our understanding of the evolutionary trajectory of the SPL gene across various species, a phylogenetic analysis was conducted on a set of 90 SPL proteins, including those from *T. kok-saghyz* (25), *H. brasiliensis* (16), *E. ulmoides* (13), *Arabidopsis thaliana* (17) and *Oryza sativa* (19). The analysis categorized these proteins into eight distinct groups, as shown in Figure 1.

The results showed that in the phylogenetic tree (I–VIII), 90 SPL genes were divided into 8 subfamilies. Their agreement with the AtSPL and OsSPL protein classification groups implies that SPL genes have been highly conserved throughout molecular evolution. SPL genes of *T. kok-saghyz* and *Arabidopsis thaliana* are distributed in all eight subfamilies, while SPL genes of *E. ulmoides* and *H. brasiliensis* are lacking in subfamily II and SPL genes of *Oryza sativa* are lacking in subfamily VIII. Subfamily VII had the most individuals (17 SPLs) out of the eight subfamilies, while subfamily II only had seven SPLs. The phylogenetic tree also revealed that a number of SPL genes from the five species clustered together, with a support rating of $\geq$70.

Table 1. Analysis of basic physical and chemical properties of 54 SPLs.

Gene	Gene ID	Chr ID	Gene Range	Exon	Intron	CDS	UTR	Size/aa	MW/kD	PI	Instability Index
TkSPL1	GWHPBCHF001261	GWHBCHF00000001	14822969:14828316	12	11	11	3	927	103,394.48	6.2	53.89
TkSPL2	GWHPBCHF002675	GWHBCHF00000002	2073280:2078116	11	10	10	3	748	83,959.66	5.95	58.08
TkSPL3	GWHPBCHF006473	GWHBCHF00000002	100814431:100818025	4	3	4	0	261	29,108.21	7.73	74.85
TkSPL4	GWHPBCHF019170	GWHBCHF00000004	830539:832919	3	2	2	3	302	34,271.32	9.08	68.14
TkSPL5	GWHPBCHF020579	GWHBCHF00000004	30786520:30796342	5	4	5	2	357	39,818.25	9	51.09
TkSPL6	GWHPBCHF020580	GWHBCHF00000004	30786520:30796342	5	4	4	3	349	38,902.15	9.1	51.1
TkSPL7	GWHPBCHF022201	GWHBCHF00000004	84269226:84270914	4	3	4	2	298	33,372.53	8.41	56.09
TkSPL8	GWHPBCHF023484	GWHBCHF00000004	107063807:107065169	2	1	2	2	198	22,079.54	9.24	65.76
TkSPL9	GWHPBCHF024887	GWHBCHF00000004	129182786:129185573	2	1	2	2	192	22,005.9	8.36	70.5
TkSPL10	GWHPBCHF025127	GWHBCHF00000004	132569671:132571972	3	2	3	2	298	33,497.02	8.76	53.76
TkSPL11	GWHPBCHF026791	GWHBCHF00000004	155862873:155865148	4	3	3	3	279	30,897.47	9.74	67.09
TkSPL12	GWHPBCHF028134	GWHBCHF00000005	14701253:14704746	4	3	3	3	351	37,175.07	7.61	52.58
TkSPL13	GWHPBCHF029402	GWHBCHF00000005	33473738:33478697	11	10	10	3	1042	115,521.09	8.36	56.28
TkSPL14	GWHPBCHF029413	GWHBCHF00000005	33656280:33661229	11	10	10	3	1039	115,165.69	8.36	57.09
TkSPL15	GWHPBCHF035319	GWHBCHF00000006	28696570:28698241	2	1	2	2	183	20,547.1	9.49	44.27
TkSPL16	GWHPBCHF039801	GWHBCHF00000007	11469584:11479658	5	4	5	2	357	39,883.37	9.1	53.96
TkSPL17	GWHPBCHF039802	GWHBCHF00000007	11469584:11479658	5	4	4	3	349	38,967.27	9.19	54.04
TkSPL18	GWHPBCHF040059	GWHBCHF00000007	13895402:13897881	3	2	2	3	171	19,026.37	8.94	60.4
TkSPL19	GWHPBCHF044300	GWHBCHF00000008	4487440:4488774	2	1	2	2	296	32,163.23	9.48	57.94
TkSPL20	GWHPBCHF044302	GWHBCHF00000008	4501786:4503817	3	2	2	3	261	29,845.17	7.03	73.8
TkSPL21	GWHPBCHF050461	GWHBCHF00000009	9840573:9843749	5	4	4	2	275	30,724.02	9.55	73.95
TkSPL22	GWHPBCHF052188	GWHBCHF00000009	28195236:28196956	3	2	3	2	316	35,456.72	9.36	68.57
TkSPL23	GWHPBCHF053518	GWHBCHF00000009	42852554:42856744	10	9	9	3	928	104,212.96	6.82	46.08
TkSPL24	GWHPBCHF053519	GWHBCHF00000009	42852554:42856744	9	8	9	2	924	103,871.69	6.95	45.77
TkSPL25	GWHPBCHF056162	GWHBCHF00000009	103280194:103281999	2	1	2	2	137	15,812.68	8.56	63.94
EuSPL1	GWHPAAAL001077	GWHAAAL00000030	988480:992976	11	10	11	0	178	20,179.44	9.03	55.87
EuSPL2	GWHPAAAL003913	GWHAAAL00000058	2037987:2040046	3	2	3	0	547	60,636.72	6.91	54.8
EuSPL3	GWHPAAAL004171	GWHAAAL00000080	203789:215644	2	1	2	0	369	41,404.83	8.07	72.6
EuSPL4	GWHPAAAL007895	GWHAAAL00000112	735958:741319	5	4	5	0	133	15,322.89	7.69	84.16
EuSPL5	GWHPAAAL008461	GWHAAAL00000115	1029716:1033122	5	4	5	0	968	107,979.44	7.33	57.38
EuSPL6	GWHPAAAL008647	GWHAAAL00000172	475295:476266	2	1	2	0	978	109,120.78	8.36	51.07

Table 1. *Cont.*

Gene	Gene ID	Chr ID	Gene Range	Exon	Intron	CDS	UTR	Size/aa	MW/kD	PI	Instability Index
EuSPL7	GWHPAAAL012748	GWHAAAL00000184	1290342:1300388	11	10	11	0	347	37,321.69	8.1	64.57
EuSPL8	GWHPAAAL012866	GWHAAAL00000249	1634971:1649669	12	11	12	0	875	98,038.82	6.26	58.57
EuSPL9	GWHPAAAL016673	GWHAAAL00006095	779825:852698	9	8	9	0	259	28,558.46	8.79	61.98
EuSPL10	GWHPAAAL020125	GWHAAAL00014124	1676:4668	3	2	3	0	363	38,927.58	9.01	64.09
EuSPL11	GWHPAAAL025240	GWHAAAL00017881	529023:533014	3	2	3	0	354	40,444.43	8.94	48.71
EuSPL12	GWHPAAAL026381	GWHAAAL00020293	536331:540436	3	2	3	0	696	77,869.21	8.88	53.91
EuSPL13	GWHPAAAL026606	GWHAAAL00026424	227394:229146	3	2	3	0	131	15,166.23	10.47	72.74
HbSPL1	GT021460.t1	CM021228.1	13875757:13877545	2	1	2	0	531	57,107.57	7.27	46.45
HbSPL2	GT021495.t1	CM021228.1	13970213:13972002	2	1	2	0	442	48,140.64	8.2	48.31
HbSPL3	GT010583.t1	CM021228.1	86118185:86120916	4	3	4	0	194	21,651.15	9.06	64.25
HbSPL4	GT010615.t1	CM021233.1	98164232:98172531	10	9	10	0	194	21,651.15	9.06	64.25
HbSPL5	GT017984.t1	CM021234.1	94639220:94645994	4	3	4	0	458	49,852.23	8.87	56.52
HbSPL6	GT003116.t1	CM021238.1	65041899:65062959	24	23	24	0	707	79,038.55	7.23	55.88
HbSPL7	GT030712.t1	CM021238.1	65225362:65248838	24	23	24	0	1065	117,893.71	8.75	46.86
HbSPL8	GT030809.t1	CM021239.1	12363240:12365845	3	2	3	0	1005	110,811.41	8.33	48.37
HbSPL9	GT019690.t1	CM021239.1	23400072:23405078	10	9	10	0	293	32,788.22	9.21	64.77
HbSPL10	GT039310.t1	CM021239.1	26622170:26632180	12	11	12	0	995	110,256.79	6.4	43.85
HbSPL11	GT033052.t1	CM021239.1	39504948:39506565	3	2	3	0	339	37001.37	9.5	59.73
HbSPL12	GT019861.t1	CM021240.1	72675955:72677659	3	2	3	0	686	77,405.9	5.86	55.24
HbSPL13	GT025439.t1	CM021241.1	2028142:2034204	10	9	10	0	368	41,070.02	9.44	51.55
HbSPL14	GT042310.t1	CM021241.1	27863168:27864903	3	2	3	0	862	97,241.22	6.29	47.94
HbSPL15	GT040479.t1	JAAGAX010000040.1	559530:565521	4	3	4	0	398	44,823.71	8.64	49.13
HbSPL16	GT028737.t1	JAAGAX010000040.1	620658:626675	4	3	4	0	404	44,567.07	8.41	55.27

3.2. Physicochemical Properties and Secondary and Three-Dimensional Structural Analysis

In the three rubber-producing plants, 54 SPL genes in all were found. The protein's amino acid composition ranged from 131 to 1065, its molecular weight from 15,166.23 to 117,893.71 kD, and its isoelectric point from 5.86 to 10.47 as a basic protein, and the instability index ranged from 43.85 to 84.16. With only 131 amino acids, EuSPL13 was the smallest of the 54 SPL proteins. HbSPL7, in contrast, had the most amino acids (1065), making it the biggest.

The secondary structure analyses predicted that all SPLs of the three species comprised alpha helices, extended strands, beta turns, and random coils (Table S1). The alpha helices and the random coils were the main secondary structural elements of SPLs. It was projected that TkSPL1 would localize to the plasma membrane in *T. kok-saghyz,* while TkSPL2 would localize to the cytoplasm, TkSPL9 to the chlo, and TkSPL18 to the cytoplasm. EuSPL8 was predicted to localize to the peroxisome in *E. ulmoides*. The remaining 49 SPL genes, excluding the aforementioned 5 SPL genes, are found in the nucleus. The Phyre2 sever was used to model the three-dimensional structure of the 54SPLs (Figures S9–S11). The results showed that the SPLs were mainly composed of alpha helices and random coils, and the structure ratios were consistent with the predicted secondary structures. The tertiary structures of all three rubber-producing plant SPLs proteins were very similar, and the results are shown in the accompanying figure, with the largest proportion of irregular curls, while the different protein spatial structures will determine the differences in function. In addition, 54 SPL proteins were predicted for hydrophilicity and transmembrane conditions (Figures S3–S8).

3.3. Analysis of Protein Domains and Conserved Motifs

Exon–intron distribution and conserved motifs were studied in order to further evaluate the structural characteristics of the five species (Figure 2). We selected SPL genes from two model plants (*Arabidopsis thaliana* and *Oryza sativa*) for comparison with SPL genes from the three rubber-producing plants found in this study. A phylogenetic tree with ten conserved motifs was built using sequence data from the 54 SPLs and the SPL genes from the two additional plants using the NJ method; 10 conservative motifs were designated Motif1–Motif10.

Motifs are shared by genes in the same subfamily, which causes them to group together and generate an unequal distribution of the TkSPL, HbSPL, and EuSPL genes in the evolutionary tree. The most varied motifs were found in subfamilies V and VII, while motifs 8 and 10 were frequently seen near the start and conclusion of the patterning, respectively. Additionally, we discovered that in subfamilies I and II, motif 9 was consistently distributed towards the start of the pattern, and pattern 7 was consistently distributed at the very end of patterning.

The protein sequences of AtSPL, OsSPL, and the 54 SPL sequences found during this work were aligned to determine the SBP domain; 14 conserved amino acids are found in the basic region, which is made up of 70–80 amino acids. The Zn-fingers (Zn-1 and Zn-2) are shown in green, while the bidirectional nuclear localization signal (NLS) structures are highlighted in red (Figure 3).

To define the protein structure, the multiple sequence alignment of full-length proteins was created using MEGA 11.0 software. The length of the conserved SPL domains has been aligned many times. With roughly 74 amino acid residues, the SBP domains at the SCR, RRR, and CQQC sequences were largely preserved. Both the nuclear localization signal (NLS) and the Zn-1 and Zn-2 zinc finger configurations are retained in these SPL domains. The amino acid distribution of the structural domains of the SPL genes of the three rubber-producing plants was very similar to that of *Arabidopsis* and rice, with the BASIC region consisting of 19 amino acids, 9 of which were highly conserved, and the HLH region containing 5 highly conserved amino acids.

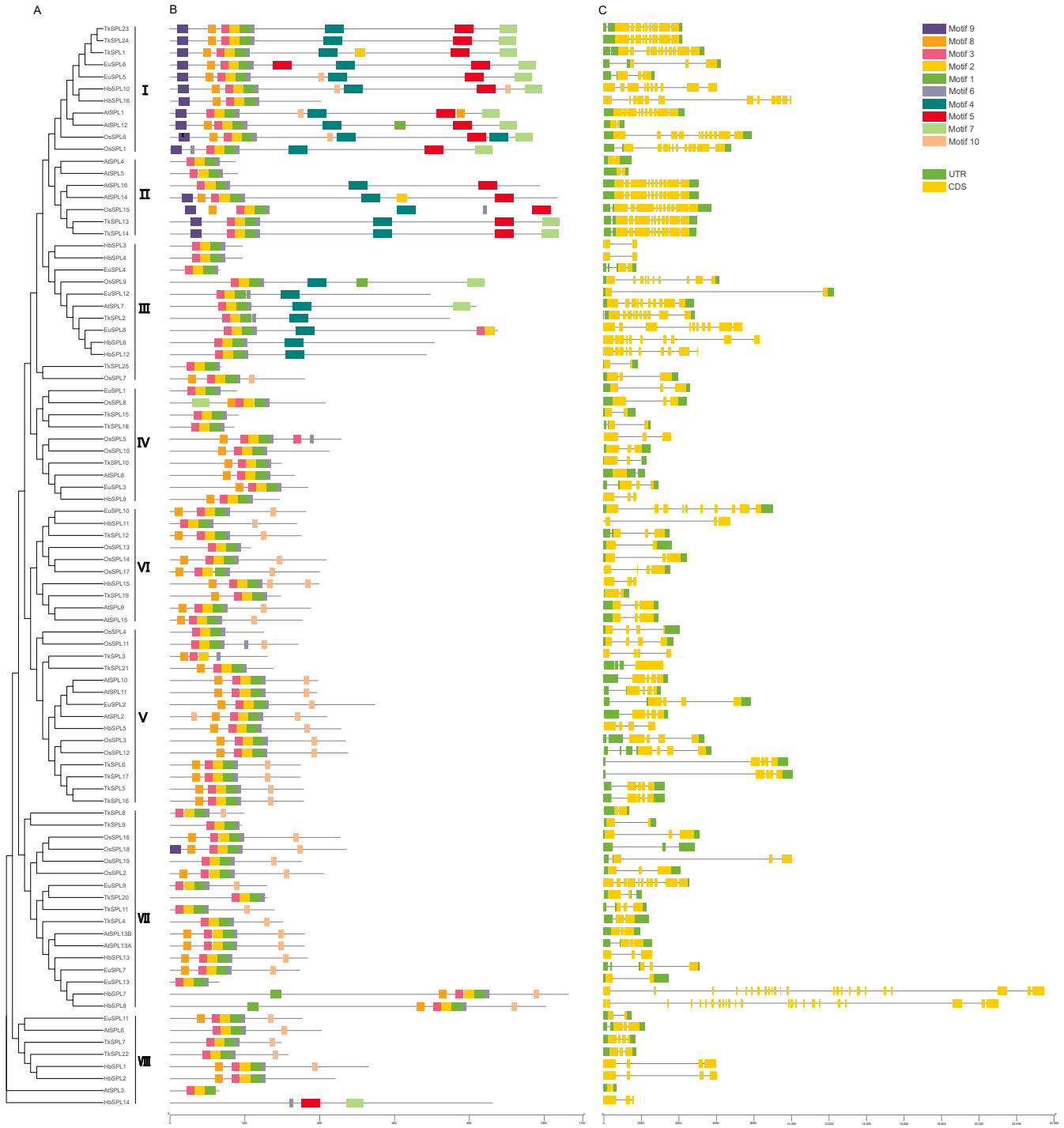

Figure 2. Analyses of protein domains and conserved motifs. (**A**) Phylogenetic tree. (**B**) Conserved motifs. (**C**) Gene structure.

3.4. Cis-Acting Elements and Collinearity Analysis

To investigate the gene functions and expression regulation patterns of EuSPLs, Plant CARE online analysis software was used to search for cis-acting elements in the 2000 bp sequences upstream of the start codon of 13 EuSPL proteins (Figure 4).

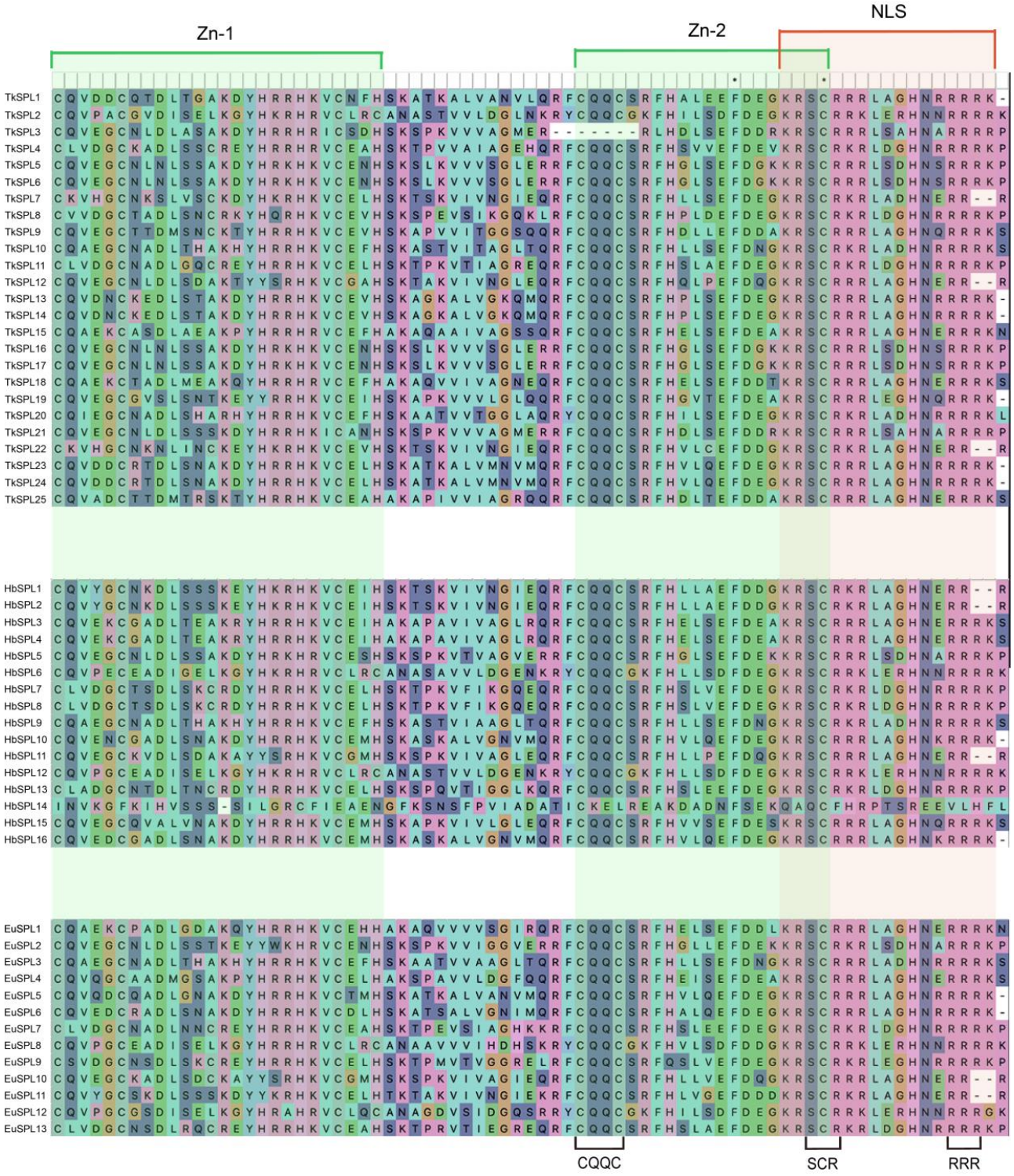

Figure 3. SBP domains from the SPL protein family with multiple sequence alignments. The symbol '*' represents a residue that is fully preserved.

Upstream of the gene coding sequence, the promoter of the gene contains a large number of cis-acting elements that can control how the gene expresses itself. The SPL promoter contains not only basic cis-acting elements but also four types of elements: (1) hormone regulatory elements, such as gibberellin response element ABRE, growth element AuxRR-core, and salicylic acid response element CGTCA-motif; (2) light response elements, such as G-Box, G-box, Box 4, GATA-motif, etc.; (3) stress response elements, like

the MBS drought stress response elements and the low-temperature response elements; and (4) physiological response elements, such as O2-site, CAT-box, etc. It is speculated that SPL genes may perform crucial functions in stress response, growth, hormone regulation, and photoperiodic regulation in *E. ulmoides*. The promoter region of EuSPLs contains 19 ABRE elements and 26 ARE elements (Figure 4B), suggesting that EuSPLs may be involved in ABA regulation and anaerobic regulation.

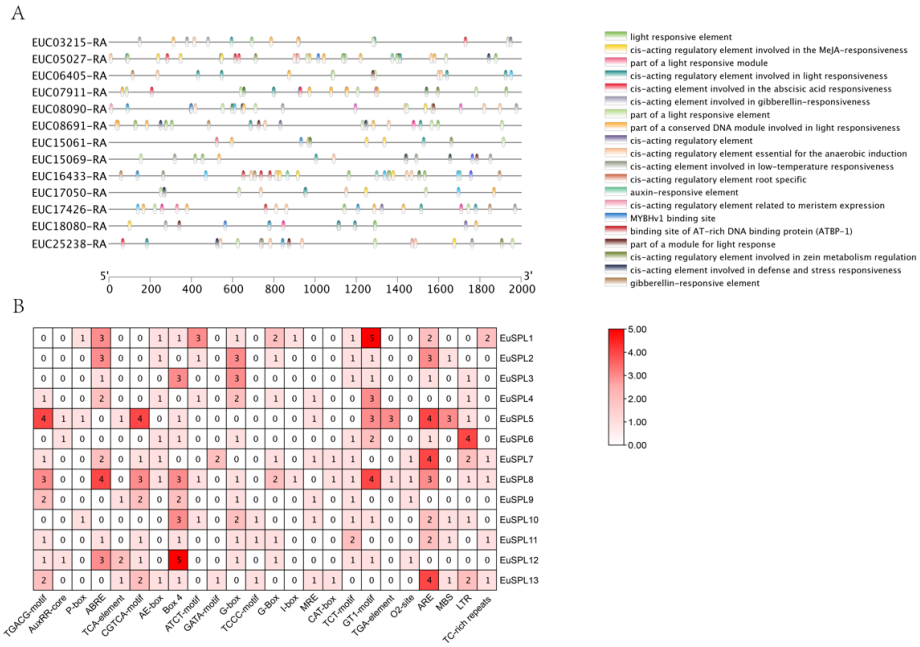

Figure 4. Cis-acting elements of the 13 EuSPLs in *E. ulmoides*: (**A**) the examination of cis-elements in SPL genes was conducted, where different cis-elements were illustrated using colored boxes; (**B**) the number of sequential elements varies, with a greater quantity of elements in darker colors.

To gain deeper insights into the evolutionary relationships, replication patterns, and evolutionary processes of the SPL genes, we created a chromosome location and collinearity plot for the 54 SPL genes (Figure 5).

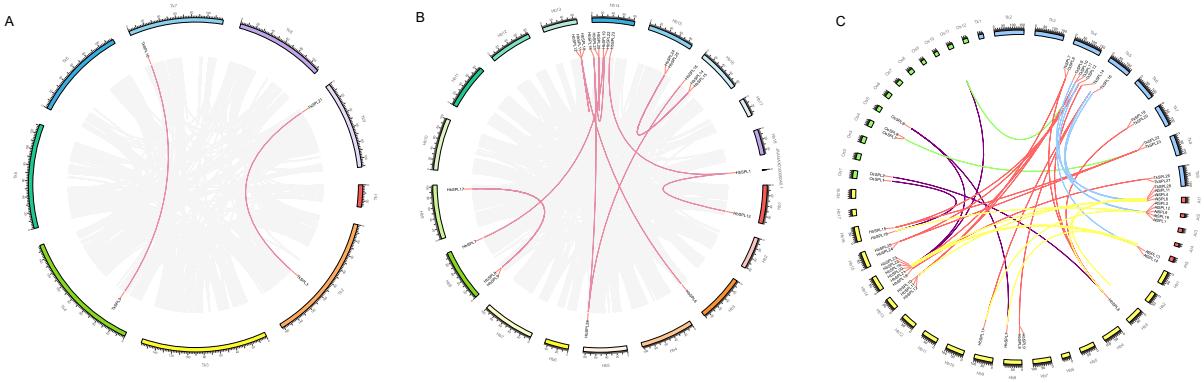

Figure 5. Collinearity analysis of rubber-producing plants. The gray line depicts all the covariates, and the colorful line depicts the pairwise replication. (**A**) *T. kok-saghyz*; (**B**) *H. brasiliensis*; (**C**) The collinearity among *H. brasiliensis*, *T. kok-saghyz*, *Oryza sativa* and *Arabidopsis thaliana*.

The tandem relationship between two species, *H. brasiliensis* and *T. kok-saghyz*, was confirmed and five and two pairs were found in their own genomes, respectively. The number of homologous SPLs of AtSPLs and OsSPLs in HbSPLs was more than that in TkSPLs. Between AtSPLs and HbSPLs, there were nine lines, but only five lines between

AtSPLs and TkSPLs. Between OsSPLs and HbSPLs, there are five lines, yet just two lines separate OsSPLs from TkSPLs. There were the most connections between *T. kok-saghyz* and *H. brasiliensis* (15).

3.5. Analysis of Expression Patterns across Several Developmental Stages and Tissue Types

According to transcriptome data, the expression pattern of the EuSPLs gene was found in order to examine the role of the SPL gene in various developmental stages and tissues of *E. ulmoides*.

Based on transcriptome data, the expression patterns were analyzed in order to analyze the roles of the EuSPLs and TkSPLs genes throughout various developmental phases and rubber production, and the gene numbers shown in the figure are consistent with the gene naming in the article (Figures 6 and 7). Low levels of expression of the majority of the EuSPLs genes were observed, but two EuSPLs genes (EuSPL5 and EuSPL6) were expressed in high abundance in all parts of *E. ulmoides* at all stages of development. Otherwise, EuSPL3 and EuSPL7 were significantly expressed in fruit, EuSPL4 was highly expressed in fruit and leaf, and EuSPL8 was highly expressed in bark.

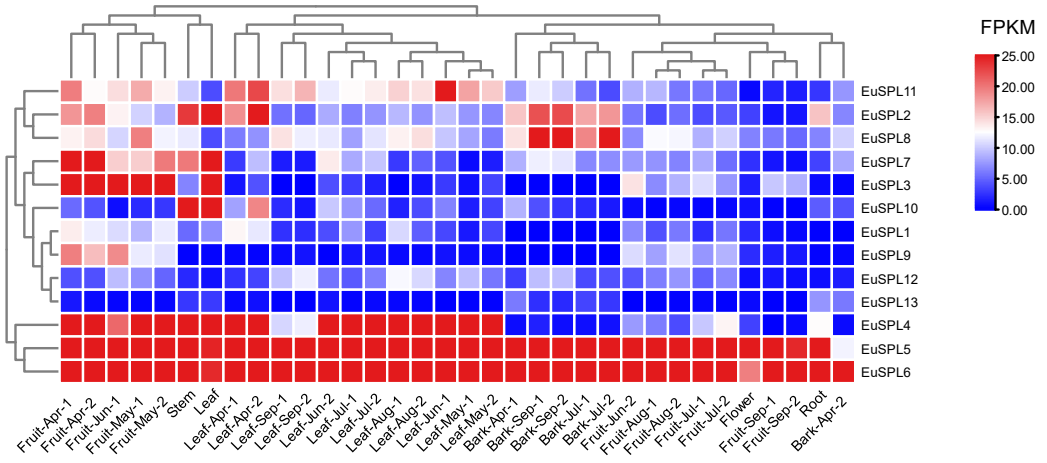

Figure 6. Patterns of gene expression for EuSPLs in various *E. ulmoides* tissue sections at various developmental stages.

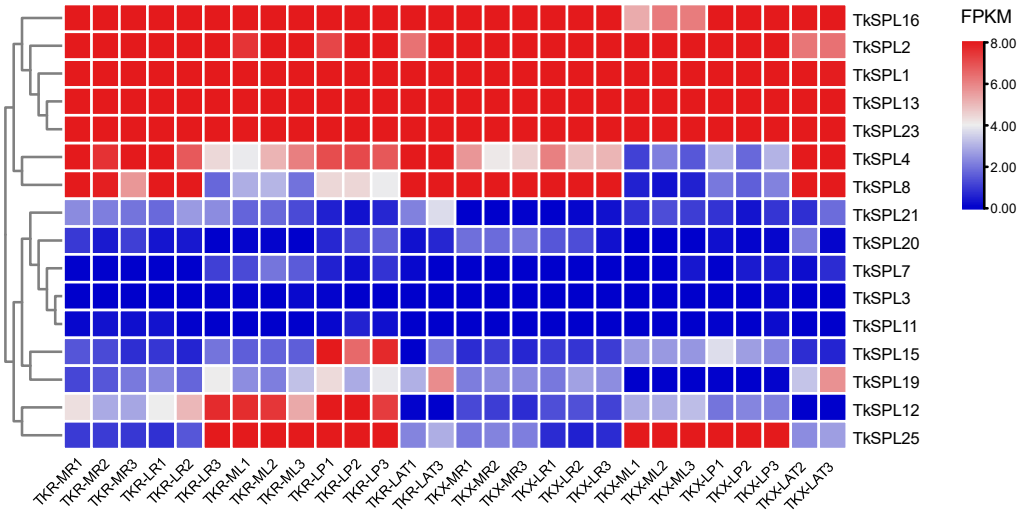

Figure 7. Patterns of gene expression for TkSPLs in various *T. kok-saghyz* tissue sections. TKX: varieties with lower rubber yield; TKR: varieties with intermediate rubber yield; MR: main roots; LR: lateral roots; ML: mature leaf; LP: leaf petiole; LAT: latex.

In *T. kok-saghyz*, several genes including TkSPL16, TkSPL2, TkSPL1, TkSPL13, and TkSPL23 show relatively high expression levels in multiple tissues. TkSPL4 and TkSPL8

exhibit high expression levels specifically in main roots, lateral roots, and latex. TkSPL25 demonstrates higher expression levels in mature leaves and leaf petioles. Furthermore, TkSPL12 shows higher expression levels in mature leaves and leaf petioles of TKR.

4. Discussion

This is the first account of a simultaneous investigation of three SPL gene families from rubber-producing plants at the genome-wide level. These findings advance our comprehension of the biological role of the SPL gene as well as the underlying molecular mechanisms.

4.1. SPL Identification across the Genome and Phylogenetic Analysis

Plant-specific TFs called SPL proteins have a structural domain of the SBP that is highly conserved [48,49], and it plays a critical role in stress response and plant growth and development [7,50,51]. Natural rubber has important economic and strategic values, and the in-depth study of rubber-producing plants is of great significance. The identification and characterization of SPL genes in numerous plants, including *Arabidopsis thaliana* [49], *Oryza sativa* [52], and *Camellia sinensis* [53], has been made possible by the quick advancement of genome sequencing technologies. However, the association of the SPL gene family in these three rubber-producing plants is not so clear that the related research is necessary and urgent.

The number of SPL members is unaffected by the size of the genome [54]. In the study, 54 SPL sequences, including 25 TkSPLs, 16 HbSPLs, and 13 EuSPLs were identified. The prediction of the physicochemical properties of SPLs showed that most of the members were basic hydrophobic proteins. The majority of the SPL proteins from the three rubber-producing plants are high in basic amino acids, which may be important in acidic subcellular settings. By bioinformatic analysis of SPL genes from three rubber-producing plants, we found that the number of SPL members in *T. kok-saghyz* was higher than that in *H. brasiliensis* and *E. ulmoides*. However, the species *T. kok-saghyz* and *E. ulmoides* shared greater similarities in terms of the number of exons, introns, and CDS as well as the number of amino acids and molecular weight.

4.2. Analysis of Protein Domains and Conserved Motifs

The predicted motifs, conserved domains, and tertiary structures show that all members have typical SBP domains and that the tertiary structures are similar. Eight groups were formed from the evolutionary examination of three rubber-producing plants, and each group had at least one gene from each of the other two plant species (*Arabidopsis thaliana* and *Oryza sativa*). It suggests that the AtSPLs and OsSPLs shared a high homology of similarity with the SPLs of three rubber-producing plants. In addition, the phylogenetic tree revealed that several SPL genes from the five species clustered together tightly (bootstrap support 70) (Figure 1). This suggests that SPL genes are functionally conserved across multiple plant species and these proteins may be orthologous [49,55], and as a result, may share similar biological roles. Sequence alignment showed that the 54 SPL genes of the three rubber-producing plants had high similarity to the structural domains of *Arabidopsis* and rice SPL proteins. According to Motif analysis, it was found that the Motif 1 motif was found to be present in all SPL transcription factors, indicating that they all belong to the SPL transcription factor family and are relatively conserved during gene evolution. Analysis of cis-acting elements revealed that EuSPL contains a large number of response elements related to hormone, light response, stress and physiology; therefore, SPL genes may play important roles in growth and development, stress response, hormone regulation and photoperiodic regulation in *E. ulmoides*.

4.3. Analysis of Responses and Expression Patterns

Plant growth and development depend heavily on hormonal cues and environmental changes [56–58]. SPL genes may play a substantial role in the control of photoperiodic,

hormone, growth, and responses to stress in three rubber-producing plants. The majority of the members of this family respond to a range of hormones and stresses, which in our study's investigation of cis-acting regions upstream of the EuSPLs promoter revealed (Figure 6) that PavSPLs may be regulated by light, stresses, and phytohormones. As with studies in other species, there have been cases that have not yet been assembled at the chromosomal level (Figure 5A) [59]. Previous studies have shown that transcriptional-level analysis can identify genes involved in plant regulation [60]. Therefore, this study aims to obtain key SPL genes involved in the growth regulation of rubber-producing plants through transcriptome analysis. Based on transcriptome data, low levels of expression of the majority of the EuSPLs genes were observed, but two EuSPLs genes (EuSPL5 and EuSPL6) were expressed in high abundance in all parts of *E. ulmoides* at all stages of development. Due to the latex production primarily occurring in the roots of *T. kok-saghyz*, it is observed that TkSPL4 and TkSPL8 show higher expression levels in the main roots, lateral roots, and latex. Therefore, it is speculated that these two genes, TkSPL4 and TkSPL8, may have a strong correlation with the latex production process in *T. kok-saghyz*. To better understand how these EuSPL and TkSPL genes regulate the response, the analyses and research of other taxa will provide tests of our perspective that are essential to the molecular mechanism of the related gene families in rubber-producing plants.

5. Conclusions

This work combines genome-wide data from three rubber-producing plants to conduct a comprehensive bioinformatics investigation of the SPL transcription factor family. A total of 54 SPL transcription factor family genes were identified and classified into eight groups based on evolutionary tree analysis. The members of the SPL family exhibit the typical SBP structural domains. Furthermore, a thorough analysis of the gene structure, conserved domain, chromosome location, cis-acting element, and expression pattern of the SPL genes in the three rubber-producing plants was conducted. Additionally, the expression patterns of the EuSPLs gene family were analyzed, revealing that the EuSPL8 gene was highly expressed in bark, EuSPL3 and EuSPL7 were highly expressed in fruit, and EuSPL4 was highly expressed in both fruit and leaf. This article focuses on the genome-wide investigation of SPL gene families in rubber-producing plants. These findings will facilitate a better understanding of the biological function and molecular mechanisms of SPL genes in rubber-producing plants.

Supplementary Materials: The following supporting information can be downloaded at: https://www.mdpi.com/article/10.3390/d15090983/s1, Table S1: predicted secondary structure and subcellular location of SPLs of three species; Figure S1: SPL domains of three rubber-producing plants; Figure S2: locations of SPL genes in three rubber-producing plants; Figure S3–S5: transmembrane situation of 13 EuSPLs, 16 HbSPLs, and 25 TkSPLs; Figure S6–S8: hydrophilicity index plot of 13 EuSPLs, 16 HbSPLs, and 25 TkSPLs; Figure S9–S11: three-dimensional structure of 13 EuSPLs, 16 HbSPLs, and 25 TkSPLs.

Author Contributions: J.W. conceived and designed the experiment. R.S. carried out bioinformatics analysis. R.S., G.A. and Y.Y. co-wrote the manuscript. J.W. and B.Y. revised the manuscript. All authors have read and agreed to the published version of the manuscript.

Funding: This work was supported by the National Key Research and Development Program of China (No. 2021YFA1300401), Guizhou University Introduction of Talents Research Project (2021, No. 6), and the specific research fund of the Innovation Platform for Academicians of Hainan Province (2022YSCXTD0005).

Institutional Review Board Statement: Not applicable.

Data Availability Statement: The data and code supporting the current study are available from the first author or corresponding author upon request.

Acknowledgments: We are very grateful to Xuchu Wang for his helpful suggestions and funding support of this research.

Conflicts of Interest: The authors declare no conflict of interest.

References

1. Yamasaki, K.; Kigawa, T.; Inoue, M.; Tateno, M.; Yamasaki, T.; Yabuki, T.; Aoki, M.; Seki, E.; Matsuda, T.; Nunokawa, E.; et al. A novel zinc-binding motif revealed by solution structures of DNA-binding domains of *Arabidopsis* SBP-family transcription factors. *J. Mol. Biol.* **2004**, *337*, 49–63. [CrossRef]
2. Klein, J.; Saedler, H.; Huijser, P. A new family of DNA binding proteins includes putative transcriptional regulators of the *Antirrhinum majus* floral meristem identity gene *SQUAMOSA*. *Mol. Gen. Genet.* **1996**, *250*, 7–16. [CrossRef]
3. Sun, Y.; Wang, Y.; Xiao, Y.; Zhang, X.; Du, B.; Turupu, M.; Wang, C.; Yao, Q.; Gai, S.; Huang, J.; et al. Genome-Wide Identification of the SQUAMOSA Promoter-Binding Protein-like (SPL) Transcription Factor Family in Sweet Cherry Fruit. *Int. J. Mol. Sci.* **2023**, *24*, 2880. [CrossRef]
4. Zhao, H.; Cao, H.; Zhang, M.; Deng, S.; Li, T.; Xing, S. Genome-Wide Identification and Characterization of SPL Family Genes in *Chenopodium quinoa*. *Genes* **2022**, *13*, 1455. [CrossRef]
5. Lai, D.; Fan, Y.; Xue, G.; He, A.; Yang, H.; He, C.; Li, Y.; Ruan, J.; Yan, J.; Cheng, J. Genome-wide identification and characterization of the SPL gene family and its expression in the various developmental stages and stress conditions in foxtail millet (*Setaria italica*). *BMC Genom.* **2022**, *23*, 389. [CrossRef]
6. Yamaguchi, A.; Wu, M.F.; Yang, L.; Wu, G.; Poethig, R.S.; Wagner, D. The microRNA-regulated SBP-Box transcription factor SPL3 is a direct upstream activator of LEAFY, FRUITFULL, and APETALA1. *Dev. Cell* **2009**, *17*, 268–278. [CrossRef]
7. Gandikota, M.; Birkenbihl, R.P.; Hohmann, S.; Cardon, G.H.; Saedler, H.; Huijser, P. The miRNA156/157 recognition element in the 3′ UTR of the *Arabidopsis* SBP box gene SPL3 prevents early flowering by translational inhibition in seedlings. *Plant J.* **2007**, *49*, 683–693. [CrossRef]
8. Zhang, Y.; Schwarz, S.; Saedler, H.; Huijser, P. SPL8, a local regulator in a subset of gibberellin-mediated developmental processes in *Arabidopsis*. *Plant Mol. Biol.* **2007**, *63*, 429–439. [CrossRef]
9. Yamasaki, H.; Hayashi, M.; Fukazawa, M.; Kobayashi, Y.; Shikanai, T. SQUAMOSA Promoter Binding Protein-Like7 Is a Central Regulator for Copper Homeostasis in *Arabidopsis*. *Plant Cell* **2009**, *21*, 347–361. [CrossRef]
10. Kropat, J.; Tottey, S.; Birkenbihl, R.P.; Depege, N.; Huijser, P.; Merchant, S. A regulator of nutritional copper signaling in *Chlamydomonas* is an SBP domain protein that recognizes the GTAC core of copper response element. *Proc. Natl. Acad. Sci. USA* **2005**, *102*, 18730–18735. [CrossRef]
11. Chen, W.W.; Jin, J.F.; Lou, H.Q.; Liu, L.; Kochian, L.V.; Yang, J.L. LeSPL-CNR negatively regulates Cd acquisition through repressing nitrate reductase-mediated nitric oxide production in tomato. *Planta* **2018**, *248*, 893–907. [CrossRef] [PubMed]
12. Zhang, L.; Ding, H.; Jiang, H.; Wang, H.; Chen, K.; Duan, J.; Feng, S.; Wu, G. Regulation of cadmium tolerance and accumulation by miR156 in *Arabidopsis*. *Chemosphere* **2020**, *242*, 125168. [CrossRef] [PubMed]
13. Cui, L.G.; Shan, J.X.; Shi, M.; Gao, J.P.; Lin, H.X. The miR156-SPL9-DFR pathway coordinates the relationship between development and abiotic stress tolerance in plants. *Plant J.* **2014**, *80*, 1108–1117. [CrossRef]
14. Wang, J.; Ye, Y.; Xu, M.; Feng, L.; Xu, L.A. Roles of the SPL gene family and miR156 in the salt stress responses of tamarisk (*Tamarix chinensis*). *BMC Plant Biol.* **2019**, *19*, 370. [CrossRef] [PubMed]
15. Dong, H.; Yan, S.; Jing, Y.; Yang, R.; Zhang, Y.; Zhou, Y.; Zhu, Y.; Sun, J. MIR156-Targeted SPL9 Is Phosphorylated by SnRK2s and Interacts With ABI5 to Enhance ABA Responses in *Arabidopsis*. *Front. Plant Sci.* **2021**, *12*, 708573. [CrossRef] [PubMed]
16. Ma, Y.; Xue, H.; Zhang, F.; Jiang, Q.; Yang, S.; Yue, P.; Wang, F.; Zhang, Y.; Li, L.; He, P.; et al. The miR156/SPL module regulates apple salt stress tolerance by activating MdWRKY100 expression. *Plant Biotechnol. J.* **2021**, *19*, 311–323. [CrossRef]
17. Schwarz, S.; Grande, A.V.; Bujdoso, N.; Saedler, H.; Huijser, P. The microRNA regulated SBP-box genes SPL9 and SPL15 control shoot maturation in *Arabidopsis*. *Plant Mol. Biol.* **2008**, *67*, 183–195. [CrossRef]
18. Wang, J.W.; Schwab, R.; Czech, B.; Mica, E.; Weigel, D. Dual effects of miR156-targeted SPL genes and CYP78A5/KLUH on plastochron length and organ size in *Arabidopsis thaliana*. *Plant Cell* **2008**, *20*, 1231–1243. [CrossRef]
19. Wang, L.; Yu, P.; Lyu, J.; Hu, Y.; Han, C.; Bai, M.Y.; Fan, M. BZR1 physically interacts with SPL9 to regulate the vegetative phase change and cell elongation in *Arabidopsis*. *Int. J. Mol. Sci.* **2021**, *22*, 10415. [CrossRef]
20. Wu, G.; Poethig, R.S. Temporal regulation of shoot development in *Arabidopsis thaliana* by miR156 and its target SPL3. *Development* **2006**, *133*, 3539–3547. [CrossRef]
21. Wu, G.; Park, M.Y.; Conway, S.R.; Wang, J.W.; Weigel, D.; Poethig, R.S. The sequential action of miR156 and miR172 regulates developmental timing in *Arabidopsis*. *Cell* **2009**, *138*, 750–759. [CrossRef] [PubMed]
22. Yu, N.; Niu, Q.W.; Ng, K.H.; Chua, N.H. The role of miR156/SPLs modules in *Arabidopsis* lateral root development. *Plant J.* **2015**, *83*, 673–685. [CrossRef] [PubMed]
23. Yu, N.; Cai, W.J.; Wang, S.; Shan, C.M.; Wang, L.J.; Chen, X.Y. Temporal control of trichome distribution by microRNA156-targeted SPL genes in *Arabidopsis thaliana*. *Plant Cell* **2010**, *22*, 2322–2335. [CrossRef] [PubMed]
24. Xue, X.Y.; Zhao, B.; Chao, L.M.; Chen, D.Y.; Cui, W.R.; Mao, Y.B.; Wang, L.J.; Chen, X.Y. Interaction between two timing microRNAs controls trichome distribution in *Arabidopsis*. *PLoS Genet.* **2014**, *10*, e1004266. [CrossRef]
25. Ioannidi, E.; Rigas, S.; Tsitsekian, D.; Daras, G.; Alatzas, A.; Makris, A.; Tanou, G.; Argiriou, A.; Alexandrou, D.; Poethig, S.; et al. Trichome patterning control involves TTG1 interaction with SPL transcription factors. *Plant Mol. Biol.* **2016**, *92*, 675–687. [CrossRef]

26. Nodine, M.D.; Bartel, D.P. MicroRNAs prevent precocious gene expression and enable pattern formation during plant embryogenesis. *Genes Dev.* **2010**, *24*, 2678–2692. [CrossRef]
27. Martin, R.C.; Asahina, M.; Liu, P.-P.; Kristof, J.R.; Coppersmith, J.L.; Pluskota, W.E.; Bassel, G.W.; Goloviznina, N.A.; Nguyen, T.T.; Martínez-Andújar, C.; et al. The regulation of post-germinative transition from the cotyledon- to vegetative-leaf stages by microRNA-targeted Squamosa Promoter-Binding Protein LIKE13 in *Arabidopsis*. *Seed Sci. Res.* **2010**, *20*, 89–96. [CrossRef]
28. Miura, K.; Ikeda, M.; Matsubara, A.; Song, X.J.; Ito, M.; Asano, K.; Matsuoka, M.; Kitano, H.; Ashikari, M. OsSPL14 promotes panicle branching and higher grain productivity in rice. *Nat. Genet.* **2010**, *42*, 545–549. [CrossRef]
29. Jiao, Y.; Wang, Y.; Xue, D.; Wang, J.; Yan, M.; Liu, G.; Dong, G.; Zeng, D.; Lu, Z.; Zhu, X.; et al. Regulation of OsSPL14 by OsmiR156 defines ideal plant architecture in rice. *Nat. Genet.* **2010**, *42*, 541–544. [CrossRef]
30. Wang, S.; Wu, K.; Yuan, Q.; Liu, X.; Liu, Z.; Lin, X.; Zeng, R.; Zhu, H.; Dong, G.; Qian, Q.; et al. Control of grain size, shape and quality by OsSPL16 in rice. *Nat. Genet.* **2012**, *44*, 950–954. [CrossRef]
31. Wang, S.; Li, S.; Liu, Q.; Wu, K.; Zhang, J.; Wang, S.; Wang, Y.; Chen, X.; Zhang, Y.; Gao, C.; et al. The OsSPL16-GW7 regulatory module determines grain shape and simultaneously improves rice yield and grain quality. *Nat. Genet.* **2015**, *47*, 949–954. [CrossRef] [PubMed]
32. Backhaus, R.A. Rubber formation in plants. *Isr. J. Bot.* **1985**, *34*, 283–293.
33. van Beilen, J.B.; Poirier, Y. Establishment of new crops for the production of natural rubber. *Trends Biotechnol.* **2007**, *25*, 522–529. [CrossRef] [PubMed]
34. Cornish, K. Alternative natural rubber crops: Why should we care? *Technol. Innov.* **2017**, *18*, 244–255. [CrossRef]
35. Wang, Y.; Guo, D.; Li, H.L.; Peng, S.Q. Characterization of HbWRKY1, a WRKY transcription factor from *Hevea brasiliensis* that negatively regulates HbSRPP. *Plant Physiol. Biochem.* **2013**, *71*, 283–289. [CrossRef] [PubMed]
36. Li, H.L.; Wei, L.R.; Guo, D.; Wang, Y.; Zhu, J.H.; Chen, X.T.; Peng, S.Q. HbMADS4, a MADS-box transcription factor from *Hevea brasiliensis*, negatively regulates HbSRPP. *Front. Plant Sci.* **2016**, *7*, 1709. [CrossRef]
37. Wang, Y.; Zhan, D.F.; Li, H.L.; Guo, D.; Zhu, J.H.; Peng, S.Q. Transcriptome-wide identification and characterization of MYB transcription factor genes in the laticifer cells of *Hevea brasiliensis*. *Front. Plant Sci.* **2017**, *8*, 1974. [CrossRef]
38. Qu, L.; Li, H.L.; Guo, D.; Zhu, J.H.; Wang, Y.; Yin, L.Y.; Peng, S.Q. HbWRKY27, a group IIe WRKY transcription factor, positively regulates HbFPS1 expression in *Hevea brasiliensis*. *Sci. Rep.* **2020**, *10*, 20639. [CrossRef]
39. Guo, D.; Yang, Z.P.; Li, H.L.; Wang, Y.; Zhu, J.H.; Peng, S.Q. The 14-3-3 protein HbGF14a interacts with a RING zinc finger protein to regulate expression of the rubber transferase gene in *Hevea brasiliensis*. *J. Exp. Bot.* **2018**, *69*, 1903–1912. [CrossRef]
40. Guo, D.; Li, H.L.; Wang, Y.; Zhu, J.H.; Peng, S.Q. A myelocytomatosis transcription factor from *Hevea brasiliensis* positively regulates the expression of the small rubber particle protein gene. *Ind. Crops Prod.* **2019**, *133*, 90–97. [CrossRef]
41. Cheng, Y.; Luo, J.; Li, H.; Wei, F.; Zhang, Y.; Jiang, H.; Peng, X. Identification of the WRKY Gene Family and Characterization of Stress-Responsive Genes in *Taraxacum kok-saghyz* Rodin. *Int. J. Mol. Sci.* **2022**, *23*, 10270. [CrossRef]
42. Zhang, H.; Gong, Y.; Sun, P.; Chen, S.; Ma, C. Genome-wide identification of CBF genes and their responses to cold acclimation in *Taraxacum kok-saghyz*. *PeerJ* **2022**, *10*, e13429. [CrossRef]
43. Liu, J.; Wang, X.; Chen, Y.; Liu, Y.; Wu, Y.; Ren, S.; Li, L. Identification, evolution and expression analysis of WRKY gene family in *Eucommia ulmoides*. *Genomics* **2021**, *113*, 3294–3309. [CrossRef]
44. Zhang, X.; Wang, X.; Pan, L.; Guo, W.; Li, Y.; Wang, W. Genome-wide identification and expression analysis of MADS-box transcription factors reveal their involvement in sex determination of hardy rubber tree (*Eucommia ulmoides* oliv). *Front. Genet.* **2023**, *14*, 1138703. [CrossRef] [PubMed]
45. Larkin, M.A.; Blackshields, G.; Brown, N.P.; Chenna, R.; McGettigan, P.A.; McWilliam, H.; Valentin, F.; Wallace, I.M.; Wilm, A.; Lopez, R.; et al. Clustal W and clustal X version 2.0. *Bioinformatics* **2007**, *23*, 2947–2948. [CrossRef] [PubMed]
46. Chen, C.; Chen, H.; Zhang, Y.; Thomas, H.R.; Frank, M.H.; He, Y.; Xia, R. TBtools: An integrative toolkit developed for interactive analyses of big biological data. *Mol. Plant* **2020**, *13*, 1194–1202. [CrossRef]
47. Bailey, T.L.; Boden, M.; Buske, F.A.; Frith, M.; Grant, C.E.; Clementi, L.; Ren, J.; Li, W.W.; Noble, W.S. MEME SUITE: Tools for motif discovery and searching. *Nucleic Acids Res.* **2009**, *37*, W202–W208. [CrossRef] [PubMed]
48. Birkenbihl, R.P.; Jach, G.; Saedler, H.; Huijser, P. Functional Dissection of the Plant-specific SBP-Domain: Overlap of the DNA-binding and Nuclear Localization Domains. *J. Mol. Biol.* **2005**, *352*, 585–596. [CrossRef]
49. Yang, Z.; Wang, X.; Gu, S.; Hu, Z.; Xu, H.; Xu, C. Comparative study of SBP-box gene family in *Arabidopsis* and rice. *Gene* **2008**, *407*, 1–11. [CrossRef]
50. Hyun, Y.; Richter, R.; Vincent, C.; Martinez-Gallegos, R.; Porri, A.; Coupland, G. Multi-layered regulation of SPL15 and cooperation with SOC1 integrate endogenous flowering pathways at the *Arabidopsis* shoot meristem. *Dev. Cell* **2015**, *37*, 254–266. [CrossRef]
51. Gao, R.; Wang, Y.; Gruber, M.Y.; Hannoufa, A. miR156/SPL10 modulates lateral root development, branching and leaf morphology in *Arabidopsis* by silencing AGAMOUS-LIKE 79. *Front. Plant Sci.* **2017**, *8*, 2226. [CrossRef]
52. Kabin, X.; Congqing, W.; Lizhong, X. Genomic organization, differential expression, and interaction of SQUAMOSA promoter-binding-like transcription factors and microRNA156 in rice. *Plant Physiol.* **2006**, *142*, 280–293. [CrossRef]
53. Zhang, D.; Han, Z.; Li, J.; Qin, H.; Zhou, L.; Wang, Y.; Zhu, X.; Ma, Y.; Fang, W. Genome-wide analysis of the SBP-box gene family transcription factors and their responses to abiotic stresses in tea (*Camellia sinensis*). *Genomics* **2020**, *112*, 2194–2202. [CrossRef] [PubMed]

54. Song, J.; Ma, D.; Yin, J.; Yang, L.; Gao, C. Genome-wide characterization and expression profiling of squamosa promoter binding protein-like (SBP) transcription factors in wheat (*Triticum aestivum* L). *Agronomy* **2019**, *9*, 527. [CrossRef]
55. Cai, C.; Guo, W.; Zhang, B. Genome-wide identification and characterization of SPL transcription factor family and their evolution and expression profiling analysis in cotton. *Sci. Rep.* **2018**, *8*, 762. [CrossRef] [PubMed]
56. Santner, A.; Calderon-Villalobos, L.I.; Estelle, M. Plant hormones are versatile chemical regulators of plant growth. *Nat. Chem. Biol.* **2009**, *5*, 301–307. [CrossRef] [PubMed]
57. Leng, P.; Yuan, B.; Guo, Y. The role of abscisic acid in fruit ripening and responses to abiotic stress. *J. Exp. Bot.* **2014**, *65*, 4577–4588. [CrossRef]
58. Guo, J.; Wang, S.; Yu, X.; Dong, R.; Li, Y.; Mei, X.; Shen, Y. Polyamines regulate strawberry fruit ripening by abscisic acid, auxin, and ethylene. *Plant. Physiol.* **2018**, *177*, 339–351. [CrossRef]
59. Duan, Q.; Li, G.-R.; Qu, Y.-P.; Yin, D.-X.; Zhang, C.-L.; Chen, Y.-S. Genome-Wide Identification, Evolution and Expression Analysis of the Glutathione S-Transferase Supergene Family in Euphorbiaceae. *Front. Plant Sci.* **2022**, *13*, 808279. [CrossRef]
60. Jaiswal, P.; Cheruku, J.R.; Kumar, K.; Yadav, S.; Singh, A.; Kumari, P.; Dube, S.C.; Upadhyaya, K.C.; Verma, P.K. Differential transcript accumulation in chickpea during early phases of compatible interaction with a necrotrophic fungus Ascochyta rabiei. *Mol. Biol. Rep.* **2012**, *39*, 4635–4646. [CrossRef]